N88-12707

Fast Autotuning of a Hydrogen Maser by Cavity Q Modulation

G. J. Dick and T. K. Tucker
Communications Systems Research Section

A new fast autotuner for the hydrogen maser has been implemented. By modulating the cavity Q, a phase shift in the maser output signal is induced which is proportional to the cavity tuning error. This phase shift is detected and fed back to a varactor tuner to stabilize the cavity against long-term drifts. Cavity Q modulation has similarities to two other autotuning methods and significant advantages over both of them. In comparison to line Q modulation, where the frequency shift induced by a change in the atomic line Q requires a second maser for detection, the high chopping frequency allowed by cavity Q modulation gives rise to a phase shift which requires only the maser's quartz crystal "flywheel" oscillator for detection. In comparison to cavity frequency modulation, statistical noise considerations are almost identical. However, a significant advantage is the lack of phase modulation of the maser output, feedback being around the null modulation condition. Furthermore, the Q modulator is a valuable analytical tool in maser alignment. Its advantage over signal injection schemes, which give somewhat lower statistical deviation, is a lack of systematic perturbations, including independence from connecting cable lengths.

We have developed and tested a PIN-diode cavity Q modulator which gives no incidental frequency shift over a very wide range of operation. Modulated at 200 Hz, it allows variations in maser cavity frequency to be compensated with a loop gain greater than 1000. Compensation of incidental amplitude modulation of the output has also been demonstrated. Calculations show that long-term stability of $3 \times 10^{-13}/\sqrt{\tau}$ *should be achievable with typical masers.*

I. General Considerations

The hydrogen maser is the most stable frequency source generally available today for all but the shortest measuring times. For very long measuring times ($\tau > 10^4$ seconds), its performance typically deteriorates as a result of frequency drift of the high-Q resonant cavity necessary to sustain oscillation. Various schemes are used to detect this drift and then to compensate for it. This can be done periodically, as part of the setup and calibration procedure, or continuously, if allowed by the procedure. Three substantially different types of autotuning methods have been proposed and implemented.

In spin-exchange autotuning, the line width or Q of the atomic hydrogen transition itself is modulated by alternating the flow of atoms into the maser cavity between two different

rates. The line width is actually broadened by both spin-exchange and electromagnetic effects. This is because while the changing density modulates the spin-exchange interaction with other atoms, changes in the rate induce variation in the RF amplitude, and thus also in the electromagnetic transition rate bandwidth. Since the Q of the atomic line determines the efficacy of any pulling of the oscillation away from its center frequency, such a frequency error will be modulated by the change in the hydrogen flow. The accuracy of compensation is just the accuracy with which the frequency difference between the two states of operation can be determined, divided by the fractional Q modulation. Measurement of this frequency difference to the highest possible accuracy takes 1000 seconds or more and requires a second maser with equivalent stability.

An advantage of this scheme is that, to the extent that the Q modulation is due to spin exchange, the frequency offset due to this same mechanism is also eliminated, giving increased accuracy to the tuned frequency. The principal disadvantages are the need for a second maser to use as a reference and the relatively long term frequency shifts that result from the modulation, making maser output unusable during the tuning process.

In signal injection autotuning [1], [2], the frequency offset of the cavity resonator is detected as a result of the difference in cavity response at two frequencies equally spaced from the maser operating frequency but far enough from it to prevent interference with it. The injected signals are generated by offsetting the frequency of the maser output signal and, theoretically, can be much larger in amplitude, allowing an excellent signal-to-noise ratio to be obtained for the inferred cavity frequency offset. The difficulty with signal injection methods is that nearly complete carrier suppression in the injected signal is required to prevent interference with maser operation. This is because phase instabilities anywhere in the receiver and electronics used to generate and transmit the injected RF signals will modulate the frequency-pulling effect of such a carrier. The resulting frequency offset of the maser output is given by

$$\frac{\delta f}{f} = \left[\frac{\left(\frac{P_c}{P_h}\right)^{1/2}}{Q_h}\right] \cdot \sin\phi \qquad (1)$$

where P_h and P_c are the hydrogen output and injected carrier powers, respectively, Q_h is the hydrogen line Q, and ϕ is the phase difference between the injected carrier and the hydrogen signal. For a line Q of 10^9 and a required frequency stability of $\delta f/f = 10^{-15}$, some combination of overall phase stability and carrier suppression of 120 dB compared to the signal power is required by Eq. (1). Since the phase of a suppressed carrier is usually not well controlled, the entire burden is placed on its magnitude. This problem has not generally been addressed by proponents of the technique.

The injected frequencies can be applied either simultaneously or sequentially. If the signals are applied together, the requirement for carrier suppression is passed on to the injection electronics in a straightforward manner. Since the main advantage of the technique is the improvement in signal-to-noise ratio that results from large injection power, a value of

$$\frac{P_i}{P_h} = 100 \qquad (2)$$

has been proposed. From Eq. (1), and for line Q and stability as above, the required carrier suppression is 140 dB.

For switched-frequency injection, some degree of carrier suppression results from the modulation index of ~10 implied by the operating conditions specified in [2]. However, this is overcome by the larger injection power which justifies the method. At its worst, with the frequency offset f_o incorrectly chosen to be an odd multiple of the modulation frequency f_m, carrier power for square-wave frequency modulation is given by

$$\frac{P_c}{P_i} = \left(\frac{2f_m}{\pi f_o}\right)^2 \qquad (3)$$

where P_i and P_c are the injected and carrier powers, giving a phase-dependent frequency variation from Eq. (1) and Eq. (2) of

$$\frac{\delta f}{f} = \frac{\left(\frac{2}{\pi}\right)\left(\frac{P_i}{P_h}\right)^{1/2}\left(\frac{f_m}{f_o}\right)}{Q_h} \qquad (4)$$

per radian of phase difference between the injected carrier and the maser oscillation. For conditions as above and a modulation index of $f_o/f_m = 11$, Eq. (4) implies a sensitivity of about $\delta f/f = 6 \times 10^{-10}$ per radian, an unacceptable value.

A much greater degree of carrier suppression *can* be accomplished by appropriately adjusting the ratio f_o/f_m. In this case, the sensitivity to frequency and duty-cycle variation and to phase variations between the switched signals will depend in detail on the ratio chosen. For example, if time spent at each frequency is chosen to be an exact multiple of the period

defined by the frequency offset ($f_o/f_m = 2N$), the sensitivity of the remaining carrier to a timing inaccuracy δt can be shown to be given by

$$\frac{P_c}{P_i} = (2 \cdot \delta t \cdot f_m)^2 \tag{5}$$

for uncontrolled phases at the two frequencies. Restating Eq. (5) in terms of duty cycle η and modulation frequency stabilities gives

$$2 \cdot \delta\eta = \frac{\delta f_m}{f_m} = \left(\frac{P_c}{P_i}\right)^{1/2} = 10^{-7} \tag{6}$$

from Eq. (1) and Eq. (2) for $Q = 10^9$ and $\delta f/f = 10^{-15}$. If the two injected frequencies could be controlled so that they were exactly in phase at the switching points, the dependence on duty cycle would be zero to the first order, a much more attractive situation. There would remain, however, a sensitivity to any AM at the switching points of the modulation cycle. These aspects indicate the complexity associated with any realistic solutions to the carrier suppression problem.

Cavity modulation autotuning [3], [4] is similar to signal injection; in both cases the electromagnetic response of the cavity to microwave signals is used to determine its frequency relative to the maser operating frequency. The difference is that instead of modulating the signal driving the cavity, some property of the cavity itself is varied. For very rapid modulations of either the cavity Q or its frequency, the output signal from the hydrogen atoms remains relatively constant, resulting in a modulation of the amplitude or phase, respectively, of the cavity output signal, even when it is perfectly tuned. If the cavity is mistuned, a complementary phase or amplitude modulation results which is proportional to the amount of mistuning. This can be detected by means of a phase-sensitive amplifier, and the signal can be used to correct the cavity frequency.

The inherent limit to performance at long averaging times for a maser stabilized in this way is determined by the phase or amplitude noise of the output signal, depending on the type of modulation used, at the modulation frequency in relation to the signal power. In this case, the autotuning power is just that available from the maser. For frequencies of interest, namely those larger than the inverse of the hydrogen response time, the noise is typically due to the follower amplifier, being identical in phase and amplitude and independent of the modulation frequency. For this reason, limits to performance are nearly identical for the two types of modulation. Furthermore, since this same source of noise dominates maser performance for short times, the performance possible from the stabilized maser can be directly related to that of the same unit at short times without stabilization. Calculation of this relationship is presented in the following section.

Systematic errors, while inherently smaller than for signal injection, determine many aspects of the design of the modulator. Because of the large modulation complementary to that being used to detect the cavity frequency deviation, any cross-modulation effects will give rise to inferred cavity frequency deviation and thus to frequency errors in the stabilized system. On the other hand, variation of the magnitude of the desired modulation causes only a change in sensitivity to frequency error. As an example, if incidental frequency modulation $\Delta_f = \delta f_c Q_c/f_c$ accompanies an intended Q-modulation $\Delta_q = \delta Q/Q_c$, a systematic change in the output frequency results which is given by

$$\frac{\delta f}{f} = \left(\frac{\Delta_f}{\Delta_q}\right) \cdot Q_h^{-1} \tag{7}$$

where Q_c is the nominal cavity Q and Q_h is the hydrogen line Q, as previously defined. Phase shifts between the modulator and cavity cause similar effects. The advantage of the modulator is that it can be constructed of a few electronic components placed directly at the maser cavity. No cable lengths need to be interposed between it and the cavity, the thermal environment is very well controlled, and the device can be designed for insensitivity to the driving signal at the designed operating points. The crucial aspects in the design of the modulator are its long-term stability and the sensitivity of incidental cross-modulation to variation in its driving signal.

To date, long-term stability measurements have been presented only for cavity frequency modulation, even though Q modulation has some substantial advantages. These include the elimination of incidental phase modulation, which is zero in the locked condition, and the availability of variable Q for calibrating and characterizing maser performance as a function of cavity Q. In a following section we present the design for such a Q modulator and results of operational tests in a hydrogen maser. The modulator uses a PIN diode as the active element and, when properly tuned, shows no incidental frequency modulation.

II. Analysis

In this section, an analysis of autotuning by cavity modulation is presented which shows that the performance of the stabilized maser can be related in a particularly simple manner to that of the same unit without stabilization for very short measuring times. This can be done because the same

additive amplifier noise limits the statistical performance in both cases. In particular, expressions are derived for the crossover time τ_c, where the $1/\tau$ performance of the unstabilized maser and the $1/\sqrt{\tau}$ performance of the stabilized maser are equal to each other. The value of τ_c for typical conditions is approximately one second. Square wave modulation is explicitly included in the treatment, since this minimizes the problem of designing out systematic errors due to cross-modulation, as will be discussed in the following section. Both Q modulation and amplitude modulation are treated, showing only small differences between them in regard to statistical properties.

The (one-sided) spectral densities of phase and amplitude fluctuation due to additive noise are equal in value and given by [5]

$$S_\phi(f) = S_{\delta\nu/\nu}(f) = \frac{kTF}{P_o} \tag{8}$$

where k is Boltzmann's constant, T the temperature, F the noise factor of the maser receiver, and P_o the output power. This power is related to the more commonly used input power from the hydrogen P_h by

$$P_o = P_h \cdot \frac{Q_e}{Q} \tag{9}$$

where Q_e is the external Q of the cavity and Q the loaded Q. The Allan variance of frequency fluctuations in the maser output due to the effect of white phase noise as shown by Eq. (8) is given by [5]

$$\sigma_y^2 = \frac{3BkTF}{8\pi^2 f_0 P_o \tau^2} \tag{10}$$

where B is the bandwidth of the measuring system and f_0 is the operating frequency. Note that this value is 3/2 times larger than the commonly used expression for the "variance" that is due to additive white noise [6] but that does not correspond to usual data-taking procedures.

The effect of this same noise on the variance of phase or fractional amplitude fluctuations is similarly given by

$$\sigma_\phi^2 = \sigma_{\delta\nu/\nu}^2 = \frac{kTF}{2P_o\tau} \tag{11}$$

This can be directly related to a necessary uncertainty in the inferred cavity frequency, due to any phase or amplitude measurement, through the slopes of phase and amplitude with respect to frequency shown in Fig. 1. The slopes indicated in the figure are the maximum in each case. For the case of phase variation it is given by

$$\frac{d_\phi}{df_c} = \frac{2Q_c}{f_0} \tag{12}$$

from which the uncertainty in cavity frequency can be derived, with

$$\sigma_{\delta f_c} = \left(\frac{f_0}{2Q_c}\right)\sigma_\phi \tag{13}$$

If the loop is closed, inferred variations in cavity frequency will cause it to be incorrectly compensated, giving variations in the operating frequency, which is pulled by the cavity mistuning. Since the pulling of the operating frequency is given by

$$\delta f_0 = \frac{\delta f_c Q_c}{Q_h} \tag{14}$$

which, together with Eq. (13), gives

$$\sigma_y = \frac{\sigma_\phi}{2Q_h} \tag{15}$$

combining with Eq. (11) gives

$$\sigma_y^2 = \frac{\sigma_\phi^2}{4Q_h^2\tau} = \frac{kTF}{8P_oQ_h^2\tau} \tag{16}$$

for the necessary variance of fractional frequency variations under closed loop conditions. The crossover between this expression, with a logarithmic slope of $-1/2$, and the unlocked maser noise given by Eq. (10) with a slope of -1, is found to be given by

$$\tau_c = \frac{3BQ_h^2}{\pi^2 f_0^2} \tag{17}$$

which for typical conditions given by B = 20 Hz, $Q_h = 10^9$, f_0 = 1.42 GHz becomes

$$\tau_c = 3.01 \text{ seconds} \tag{18}$$

Such a crossover time is shown in Fig. 2.

If the cavity were detuned so that the operating frequency lay at the point of maximum slope of the amplitude curve

shown in Fig. 1, a similar inference could be made as to necessary fluctuations in output frequency if measurement of the cavity frequency were inferred from the resulting amplitude. As in Eq. (12) we have

$$\frac{dv}{df_c} = \frac{4v_0 Q_c}{3^{3/2} f_0} \tag{19}$$

and, following an identical procedure beginning again with Eq. (11), return a value for σ_y^2 which is larger by 27/4 than that given by Eq. (16) and a value for τ_c smaller by the same factor. This gives an apparent disadvantage to the frequency-modulation technique, but one that it recovers, as is shown below.

So far, this has been a calculation in principle, since no mechanism has been included to allow a measurement of the phase of the signal from the maser cavity. Figures 3 and 4 show the phase and amplitude variations $\Delta\phi$ and ΔV which result from rapid Q and frequency modulation in the presence of an offset between the cavity frequency f_c and the operating frequency f_0. Considering the case of Q modulation explicitly, instead of Eq. (12) we write

$$\Delta\phi = \frac{2\Delta_q Q_c \Delta f_c}{f_0} \tag{20}$$

where $\Delta_q = \Delta Q_c / Q_c$ is the fractional Q modulation, and Δf_c is the frequency offset between f_0 and f_o. Combining with the pulling Eq. (14) gives, in a manner analogous to Eq. (15)

$$\sigma_y = \frac{\sigma_{\Delta\phi}}{2\Delta_q Q_h} \tag{21}$$

The variance for the phase difference $\sigma_{\Delta\phi}$ shown in Fig. 3 is also not the same as that given by Eq. (11), but it is easy to evaluate for the case of square-wave modulation. If one-half of the time is spent in each state, the value given by Eq. (11) would double, effectively taking τ to a new value $\tau/2$. The difference between two such quantities will again double the square of the variance, giving

$$\sigma_{\Delta\phi}^2 = \frac{2kTF}{P_o \tau} \tag{22}$$

which, when combined with Eq. (21), gives a value of

$$\sigma_y^2 = \frac{kTF}{2\Delta_q^2 Q_h^2 P_o \tau} \tag{23}$$

for the variance and

$$\tau_c = \frac{3B\Delta_q^2 Q_h^2}{4\pi^2 f_0^2} \tag{24}$$

for the crossover time. For $\Delta_q^2 = 2$, and the conditions as described above, a value of

$$\tau_c = 0.375 \text{ second} \tag{25}$$

is obtained.

For frequency modulation, there is an apparent value to choose for the frequency deviation; it is just that which maximizes the slope. Taking that offset (a fractional displacement of $1/[\sqrt{8Q}]$ of the cavity frequency), modulation as shown in Fig. 4 gives a signal strength of

$$\Delta v/v = \frac{8Q_c \Delta f_c}{3^{3/2} f_0} \tag{26}$$

proportional to the frequency offset Δf_c, as in Eq. (20). Again, accounting for the statistics of modulation we have

$$\sigma_{\Delta v/v}^2 = \frac{2kTF}{P_o \tau} \tag{27}$$

as in Eq. (22) and

$$\sigma_y^2 = \frac{3^3 kTF}{2^5 Q_h^2 P_o \tau} \tag{28}$$

for the variance, giving, again with Eq. (10)

$$\tau_c = \frac{4BQ_h^2}{9\pi^2 f_0^2} \tag{29}$$

for the crossover time, and

$$\tau_c = 0.447 \text{ second} \tag{30}$$

for the conditions as above, showing a slight advantage for the frequency modulation method. This would be reversed if a Q modulator could be designed which, instead of dissipating energy in the cavity, either enhanced it or transmitted it to the receiver. Variance values calculated here are somewhat higher than those estimated in [1].

The reference signal for phase measurements can be provided by a quartz crystal oscillator. As is demonstrated in Fig. 2, for times corresponding to a modulation frequency of 100 Hz the phase noise from the maser, as calculated, will be the dominant contribution to measurement uncertainty.

III. PIN Diode Modulator

Figures 5 and 6 show block and schematic diagrams of an autotuned maser using a PIN diode Q modulator. Cavity tuning was accomplished using a varicap diode external to the maser physics package. The modulator itself is placed in the vacuum space and is mounted directly on the resonant cavity itself. First tests on a test-bed maser were entirely successful, with the locked loop sustaining its operation for indefinite periods of time and for a wide variety of time constants.

In the design of the PIN-diode modulator an attempt was made to minimize as much as possible any variation of the systematic contribution of the modulator and its support equipment to the maser output frequency. To that end, it seemed necessary to use square-wave modulation; while it might be possible to make the tuning properties of the modulator insensitive to the driving conditions at the end points, it would be difficult to accomplish this throughout the range of its operation.

Figure 7 shows schematically the tuning properties of three possibly useful modulators. Of these, the curve labeled C is clearly superior, with no detuning anywhere in its range. Curve B is less desirable but still workable. It would be necessary to minimize the switching time because of detuning effects in its midrange, but equal tuning effects at its two end points mean that duty cycle sensitivity is not a problem. Curve A is clearly the worst, showing insensitivity to applied current in the highly lossy state as required but requiring careful control of the duty cycle, since frequencies at the end points are different. The zero-current state, shown at the origin, is inherently insensitive to external circuit instabilities, since the diode is in an open-circuit condition at that point. We find that, depending on its tuning, our modulator follows closely curve A or C. Its operation can be understood as follows.

If the circuit diagram for any passive device coupled to an electromagnetic resonator is redrawn in the form shown in Fig. 8, the effect of the circuit on the properties of the resonator takes a particularly simple form. In this case the loading Q_1 and frequency shift are given by

$$Q_1 = R_{\text{eff}} \cdot \frac{2\pi E_c}{(emf)^2} \tag{31}$$

and

$$\frac{\delta f}{f} = C_{\text{eff}} \cdot \frac{(emf)^2}{2E_c} \tag{32}$$

where E_c is the energy stored in the resonator and *emf* is the open circuit voltage coupled to the circuit resulting from that energy and the coupling configuration. Reduced to this form, it is apparent that frequency shifts can be seen to be due only to an effective capacitance (positive or negative), and added losses only to the effective resistance.

The equivalent circuit of the PIN modulator shown in Fig. 6 is given in Fig. 9, showing the loop inductance L_c, tuning capacitor C_t, incidental inductance L_i, and the PIN diode parameters R_p and C_p. If the capacitance C_p is a constant, the circuit as shown is sufficient to give performance C as shown in Fig. 7. This is accomplished by tuning the variable capacitor C_t so that its reactance is equal and opposite to that of the sum of the two inductances. In that case R_{eff} in Fig. 8 becomes R_p and C_{eff} becomes C_p. Since C_p is assumed constant, only a constant frequency shift results under any circumstance, and a change in R_p only affects the Q. Specifications for PIN diode parameters often show an effective parallel capacitance which has one value under back biased conditions, and another when resistive. The addition of R_t in Fig. 10 would allow compensation for such a characteristic.

We do not find any evidence of variation in C_p as the PIN diode resistance is varied by a changing current through the diode. We chose to design the modulator for "low Q" operation, with the reactances associated with L_c and C_t about equal to the loading resistance of the diode in the "on" condition. The value of this resistance is about 100 ohms. The Q of the cavity can be reduced far below its nominal "low Q" value by further reduction of R_p to 10 ohms or below. The tuning procedure is to adjust for nominally zero frequency shift in this very low Q condition where any imbalance between $L_c + L_i$ and C_t is exacerbated. Using this procedure, no tuning effects could be detected between high and low Q states of the modulator.

IV. Summary

Analysis of several types of autotuning schemes has been presented with particular attention to both statistical and systematic errors in cavity-modulation and signal injection methods. Systematic variations due to incomplete carrier suppression in signal-injection methods are found to be a very substantial difficulty, probably outweighing any statistical advantage. Statistical analysis of cavity Q- and frequency-modulation methods shows them to be essentially identical

in this regard, with limiting performance shown to be directly related to that of the unstabilized maser.

A PIN-diode Q modulator has been designed, constructed, and tested which shows no observable incidental frequency modulation. First tests on a test-bed maser were entirely successful, with the locked loop sustaining its operation for indefinite periods of time. Operation of this relatively low performance unit was not adversely affected in any way by the effects of the modulator. Further tests are under way.

Acknowledgments

We would like to acknowledge the substantial contributions to this work by R. L. Sydnor, the cooperation and support of L. Maleki and P. F. Kuhnle, and assistance with tests and data reduction by R. E. Taylor, W. A. Diener, and C. A. Greenhall.

References

[1] C. Audoin, P. Lesage, J. Viennet, and R. Barillet, "Theory of Hydrogen-Maser Auto-Tuning System Based on the Frequency or Phase Method," *IEEE Trans. Instrum. Meas.*, vol. IM-29, pp. 98–104, June 1980.

[2] C. Audoin, "Fast Cavity Auto-Tuning Systems for Hydrogen Maser," *Revue Phys. Appl.*, vol. 16, pp. 125–130, March 1981.

[3] H. E. Peters, "Design and Performance of New Hydrogen Masers Using Cavity Frequency Switching Servos," in *Proc. 38th Annual Symp. Freq. Control*, pp. 420–427, 1984.

[4] R. B. Hayes and H. T. M. Wang, "Design for a Subcompact Q-Enhanced Active Maser," in *Proc. 38th Annual Symp. Freq. Control*, pp. 80–84, 1984.

[5] "Characterization of Frequency and Phase Noise," *Recommendations and Reports of the CCIR, Fifteenth Plenary Session*, Report 580-1, p. 91, 1982.

[6] L. S. Cutler and C. L. Searle, "Some Aspects of the Theory and Measurement of Frequency Fluctuations in Frequency Standards," *Proc. IEEE*, vol. 54, pp. 136–154, February 1966.

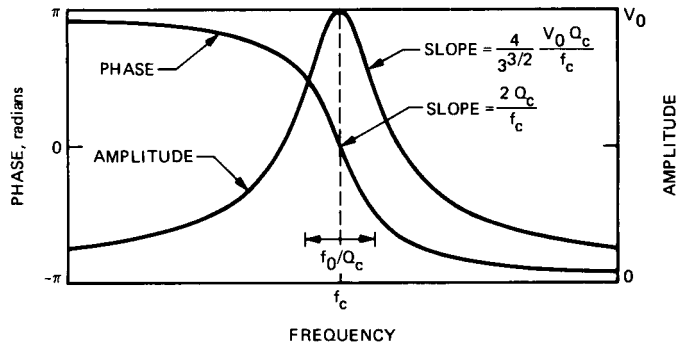

Fig. 1. Cavity frequency response

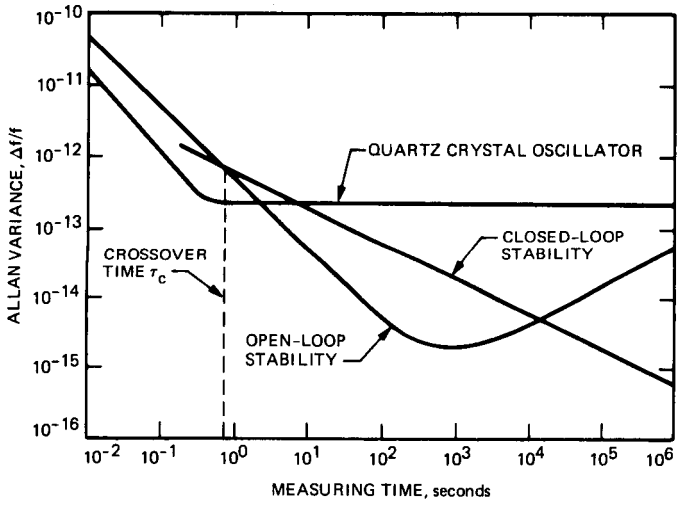

Fig. 2. Limiting performance for hydrogen maser with cavity modulation autotuning

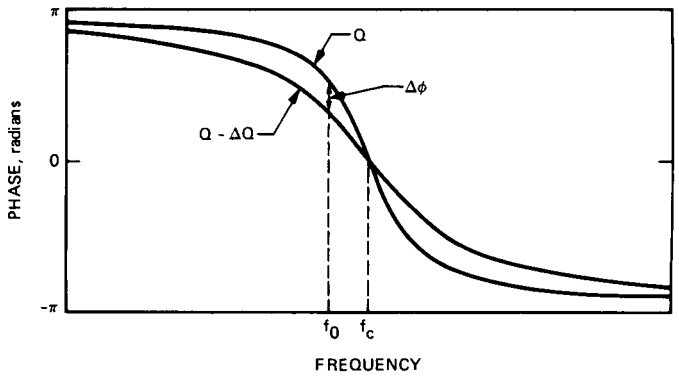

Fig. 3. Effect of Q modulation on phase response

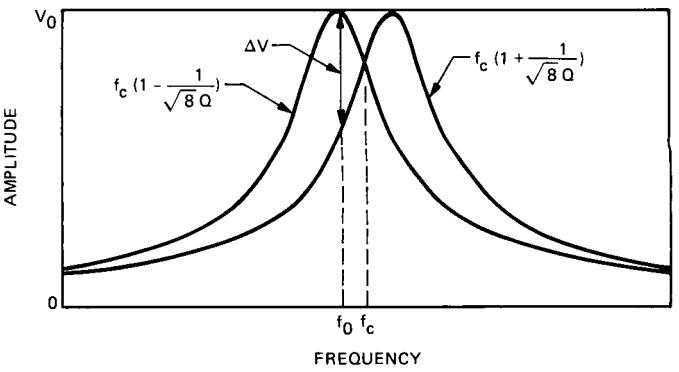

Fig. 4. Effect of frequency modulation on amplitude response

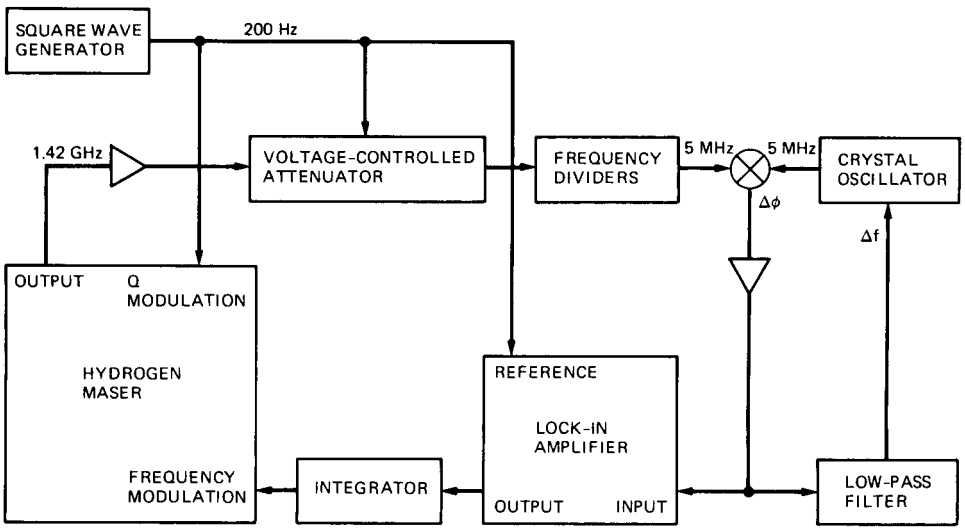

Fig. 5. Block diagram for cavity Q modulation system as tested

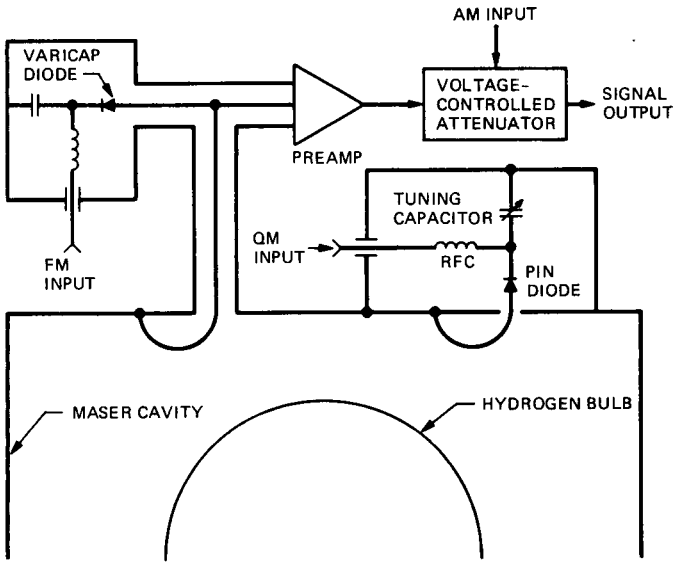

Fig. 6. Schematic diagram of Q-modulated maser

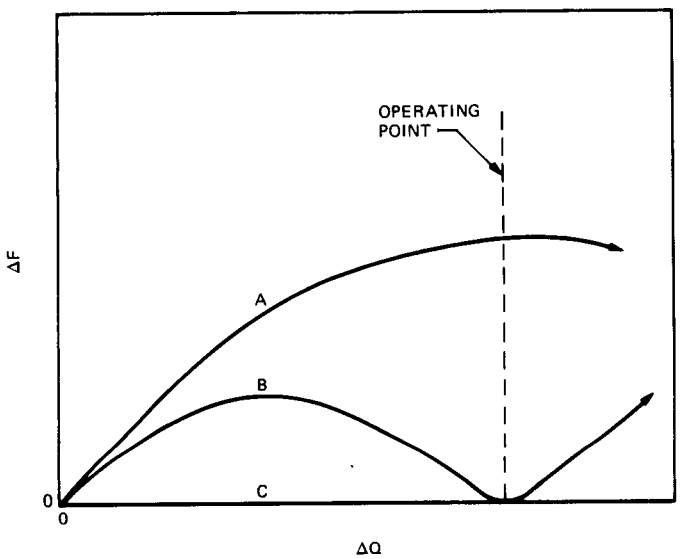

Fig. 7. Incidental frequency modulation for several usable Q modulators

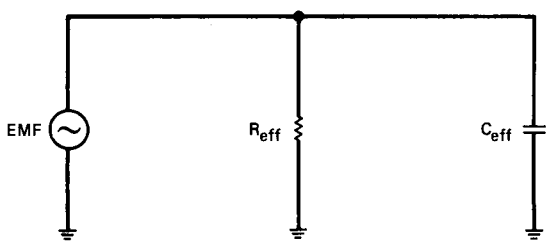

Fig. 8. Q modulator equivalent circuit

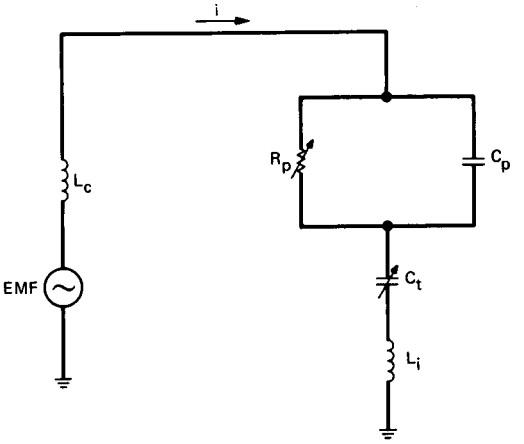

Fig. 9. Q modulator for constant C_p

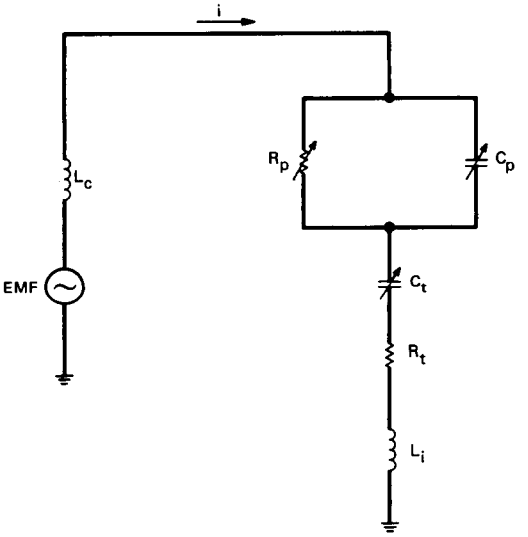

Fig. 10. Q modulator for varying C_p